

PROCESS DESIGN AND CONTROL

Comparison of Various Control Configurations for Continuous Bioreactors

Ying Zhao and Sigurd Skogestad*

Department of Chemical Engineering, Norwegian University of Science and Technology,
N-7034 Trondheim, Norway

Five control configurations for continuous bioreactors are analyzed using a simple model. A controller-independent measure, the partial disturbance gain, is used for evaluating their controllability with respect to disturbance rejection. The computation of the partial disturbance gain is generalized to the case with several uncontrolled outputs. At substrate-limited growth conditions, the concentration turbidostat using the feed substrate concentration as the manipulated variable is the best control configuration. The conventional turbidostat should be avoided. When the cell growth is not substrate limited, all these control configurations are effective except the concentration nutristat which is not feasible regardless if the growth is substrate limited or not.

1. Introduction

Bioreactor control has become an active area of research in recent years. Much emphasis has been placed on the control of fed-batch bioreactors because of their prevalence in industry traditionally. However, when production of cell mass or product is to be optimized, continuous operation is desirable.

Unforeseen disturbances in a bioreactor may result in a failure in the operation of the reactor, such as *washout*, and require a new start-up procedure. Therefore, there is a strong economic incentive to develop efficient control strategies that would enable rapid start-up and stabilization of steady states in continuous bioreactors subject to disturbances.

Problem Formulation. As already noted, the primary objective of a continuous bioreactor control system is usually to avoid having the reaction stop due to washout. This may be done by closing one feedback loop and controlling the cell mass or substrate concentrations (X or S (g/L)). In addition, in order to optimize the reaction and maintain the quality of the product, one may as a secondary control objective want to keep both X and S at some desired values. Two degrees of freedom are available for control, namely the total feed flow rate, F (L/h) (which is usually normalized with the reactor volume to get the dilution rate, $D = F/V$ (h⁻¹)), and the feed substrate concentration, S_f (g/L). We then have that the candidate inputs and outputs are

$$\mathbf{u} = \begin{bmatrix} F \\ S_f \end{bmatrix}, \quad \mathbf{y} = \begin{bmatrix} X \\ S \end{bmatrix}$$

One obvious solution is to implement a 2×2 control configuration. However, this is expensive and probably not necessary, because microorganisms have *intracellular* regulatory mechanisms, and thus there exist strong interactions between the two outputs. In this paper the main consideration is therefore whether one may achieve acceptable control performances of both

outputs by controlling only one of them. This gives rise to four possible 1×1 control configurations. Actually, there are more possibilities for selecting inputs. For example, to adjust the total feed flow rate (F), we can adjust F directly, or as in the modified turbidostat with two feed streams proposed by Agrawal and Lim (1984), we can use either the flow rate of the concentrated substrate stream (F_s) or the flow rate of the sterile water stream (F_w).

The problem described above is actually a quite general control strategy problem where one is faced with a "partial control problem", that is, to use a subset of the available inputs to control a subset of the outputs. Define $\mathbf{y} = [\mathbf{y}_1 \mathbf{y}_2]^T$ and $\mathbf{u} = [\mathbf{u}_1 \mathbf{u}_2]^T$ as shown in Figure 1.

The problem is to select the controlled outputs (\mathbf{y}_2) and the manipulated inputs (\mathbf{u}_2). Issues are:

(1) Use of \mathbf{u}_2 to control \mathbf{y}_2 should yield satisfactory control performance (\mathbf{u}_2 should have a "large" effect on \mathbf{y}_2 to avoid input constraints; delays and RHP-zeros from \mathbf{u}_2 to \mathbf{y}_2 should not conflict with the desired bandwidth needed for disturbance rejection and set-point tracking).

(2) With these control loops closed (i.e., with \mathbf{y}_2 approximately constant) and with the unused inputs \mathbf{u}_1 constant, the uncontrolled outputs \mathbf{y}_1 should be relatively insensitive to disturbances \mathbf{d} .

Issue 1 is a conventional feedback control problem where dynamic issues generally are most important, while steady-state considerations are often more important for issue 2. To evaluate both these issues the controllability analysis of the alternative structures needs to be performed. A useful tool when considering issue 2 is the partial disturbance gain proposed by Skogestad and Wolff (1992), which yields the effect of a disturbance on the uncontrolled output when the controlled outputs are kept constant. A more general definition of the partial disturbance gain will be given in section 2.

Such strategy decisions arise frequently in process control. One extensively studied problem is the control configuration selection for distillation columns (e.g.,

* E-mail: skoge@kjemi.unit.no. Fax: +47-73-594080.

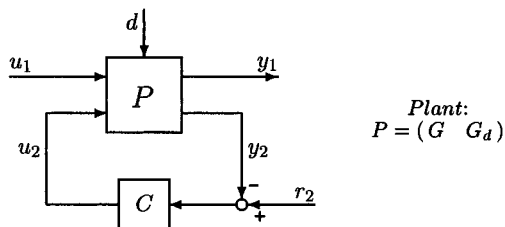


Figure 1. Simplified partial control system.

Skogestad and Morari (1987)). For distillation columns it is well-known that some configurations have better "built-in" disturbance rejection ability than others; i.e., the sensitivity of the uncontrolled outputs with respect to disturbances is less.

The issue of disturbances has not been widely discussed in the literature on the controllability analysis for bioreactors. The objective of this paper is then to make a comparison of various control configurations for continuous bioreactors on the basis of the controllability analysis with respect to disturbance rejection.

Control Configurations Studied. In this paper five control configurations are examined:

(1) Conventional turbidostat ($D \rightarrow X$ configuration). Dilution rate (D) is used to control the cell mass concentration (X).

(2) Conventional nutristat ($D \rightarrow S$ configuration). D is used to control the substrate concentration (S).

(3) Concentration turbidostat ($S_f \rightarrow X$ configuration). Feed substrate concentration (S_f) is used to control X (Menawat and Balachander, 1991).

(4) Concentration nutristat ($S_f \rightarrow S$ configuration). S_f is used to control S (Menawat and Balachander, 1991).

(5) Modified turbidostat ($D_w \rightarrow X$ configuration). Dilution rate of the sterile water stream (D_w) is used to control X (Agrawal and Lim, 1984).

Previous Work. The two most common control configurations are the turbidostat and nutristat with the dilution rate D as a manipulated input. In a turbidostat the cell mass concentration X is controlled (in practice, the optical density is used to infer X). In a nutristat the residual substrate concentration S is controlled. Edwards, Ko, and Balogh (1972) analyzed and compared these two configurations for a bioreactor with substrate inhibition kinetics, and they concluded that the nutristat is superior to the turbidostat in many applications. Agrawal and Lim (1984) evaluated the turbidostat, nutristat, and other control configurations on the basis of the local controllability, local stability, input multiplicity, and steady-state gains. They concluded that the conventional turbidostat and nutristat are feasible only at those conditions where the cell growth is not substrate limited. They then proposed a modified turbidostat with two feed streams, a sterile water stream and a stream containing the concentrated amounts of the limiting substrate and other nutrients. The dilution rate of the sterile water stream (D_w) is used as the manipulated variable with the concentrated substrate stream of constant flow (D_s). They found this modified turbidostat to be superior to the conventional turbidostat in that it can operate under all growth conditions. Menawat and Balachander (1991) proposed to use the feed substrate concentration S_f as the manipulated variable and claimed that this control configuration improves the control performance for control of either X or S compared to using the dilution rate as the manipulated variable.

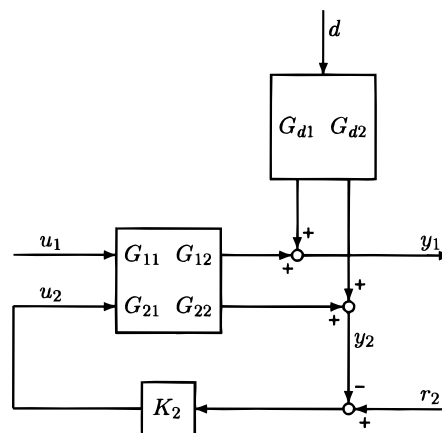


Figure 2. Block diagram of a partial control system.

2. Controllability Measure

In this paper simple frequency-dependent tools are used to study the inherent control characteristics. In particular, for selecting the "controlled" pairings we consider the open-loop disturbance gain \mathbf{G}_d , and for selecting the "uncontrolled" pairings we consider the partial disturbance gain \mathbf{P}_{d1} .

Tools. Consider a linear model of the form

$$\mathbf{y}(s) = \mathbf{G}(s) \mathbf{u}(s) + \mathbf{G}_d(s) \mathbf{d}(s) \quad (1)$$

As shown in Figure 2, we further rearrange and partition the model $\mathbf{y} = \mathbf{G}\mathbf{u} + \mathbf{G}_d\mathbf{d}$ such that the first part of \mathbf{y} contains the uncontrolled outputs (\mathbf{y}_1) and the first part of \mathbf{u} contains the unused inputs (\mathbf{u}_1), whereas the remaining outputs \mathbf{y}_2 are controlled using the remaining inputs \mathbf{u}_2 . We then have

$$\mathbf{y}_1 = \mathbf{G}_{11}\mathbf{u}_1 + \mathbf{G}_{12}\mathbf{u}_2 + \mathbf{G}_{d1}\mathbf{d} \quad (2)$$

$$\mathbf{y}_2 = \mathbf{G}_{21}\mathbf{u}_1 + \mathbf{G}_{22}\mathbf{u}_2 + \mathbf{G}_{d2}\mathbf{d} \quad (3)$$

The open-loop disturbance sensitivity for outputs \mathbf{y}_1 and a disturbance \mathbf{d} is

$$\left(\frac{\partial \mathbf{y}_1}{\partial \mathbf{d}} \right)_{\mathbf{u}} = \mathbf{G}_{d1} \quad (4)$$

The corresponding partial disturbance sensitivity for \mathbf{y}_1 with outputs \mathbf{y}_2 perfectly controlled by using \mathbf{u}_2 is defined as (Skogestad and Wolff, 1992)

$$\mathbf{P}_{d1} \stackrel{\text{def}}{=} \left(\frac{\partial \mathbf{y}_1}{\partial \mathbf{d}} \right)_{\{\mathbf{y}_2=0\} \text{ using } \{\mathbf{u}_2\}} \quad (5)$$

A simple derivation (see Appendix) yields the following expression for the partial disturbance gain,

$$\mathbf{P}_{d1} = \mathbf{G}_{d1} - \mathbf{G}_{12}\mathbf{G}_{22}^{-1}\mathbf{G}_{d2} \quad (6)$$

or alternatively (see Appendix)

$$\mathbf{P}_{d1} = ([\mathbf{G}^{-1}]_{11})^{-1}[\mathbf{G}^{-1}\mathbf{G}_d]_1 \quad (7)$$

The latter generalizes the scalar expression given by Skogestad and Wolff (1992). The partial disturbance gain yields the disturbance gain for a system under partial control. The advantage with the partial disturbance gain is that it depends only on the plant itself; i.e., the partial disturbance gain is a controller-independent controllability measure. In particular, \mathbf{P}_{d1}

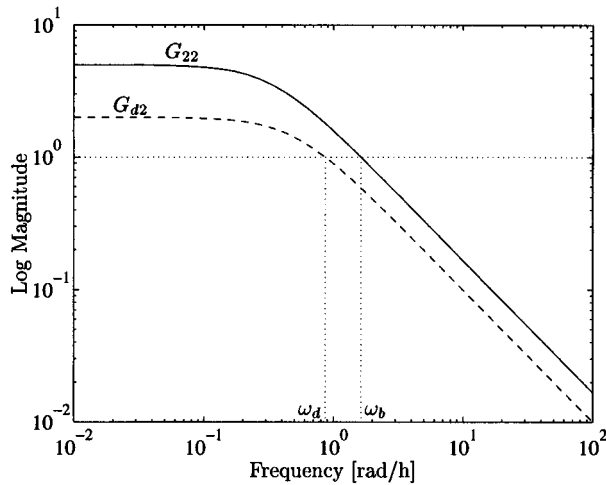


Figure 3. Analysis of "controlled" subsystem.

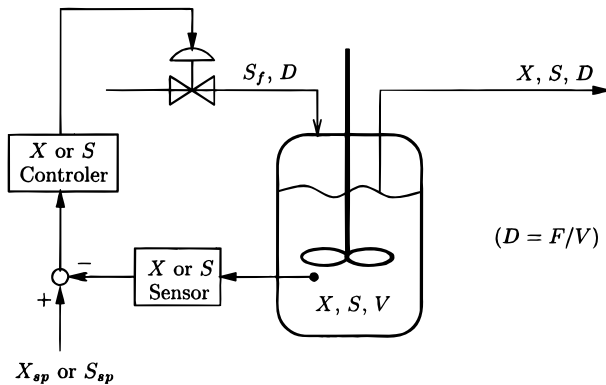


Figure 4. Schematic diagram of a continuous bioreactor.

is a vector for a single disturbance \mathbf{d} , and \mathbf{P}_{d1} is a matrix for k simultaneous disturbances $\mathbf{d} = [d_1 \cdots d_k]^T$. We use the induced 2-norm¹ of \mathbf{P}_{d1} , $\|\mathbf{P}_{d1}\|_2 = \bar{\sigma}(\mathbf{P}_{d1})$ (singular value), to evaluate the overall effect of simultaneous disturbances on uncontrolled outputs \mathbf{y}_1 . Note that $\|\mathbf{A}\|_2$ is equal to $\|\mathbf{A}\|_2$ (Euclidean norm) when \mathbf{A} is a vector, so for simplicity we use $\|\mathbf{A}\|_2$ throughout the paper both when \mathbf{A} is a matrix or vector.

Summary of Controllability Analysis. The variables should first be scaled with respect to their allowed or expected range such that all variables are less than 1 in magnitude (norm). The objective of the controllability analysis in this paper is to find the best partial control configuration, that is, to select the controlled outputs (\mathbf{y}_2) (and inputs \mathbf{u}_2) such that the norm of \mathbf{P}_{d1} , $\|\mathbf{P}_{d1}\|_2$ is small, at least we want $\|\mathbf{P}_{d1}\|_2$ smaller than $\|\mathbf{G}_{d1}\|_2$. The controllability analysis then consists of two main steps:

(1) Analysis of "controlled" subsystem with "controlled pairing" \mathbf{u}_2 - \mathbf{y}_2 (see Figure 3).

(a) To get the acceptable speed of response: Prefer pairings for which \mathbf{G}_{22} has no delays and RHP-zeros within the desired bandwidth range. The desired frequency bandwidth ω_b should be larger than the frequency range ω_d where for some disturbance \mathbf{d} , $\|\mathbf{G}_{d2}(j\omega)\|_2 > 1$; i.e., we want $\omega_b \geq \omega_d$.

(b) To avoid input constraints: Prefer pairings for which $\|\mathbf{G}_{22}^{-1}\mathbf{G}_{d2}\|_2 \leq 1$ so that $\|\mathbf{u}_2\|_2 \leq 1$ (by setting $\mathbf{u}_1 = 0$ in eq 29 in the Appendix) within the desired bandwidth range even under the worst case where $\|\mathbf{d}\|_2 = 1$.

(2) Analysis of "uncontrolled" subsystem with "uncontrolled pairing" \mathbf{u}_1 - \mathbf{y}_1 . To get acceptable disturbance sensitivity for the uncontrolled outputs: Prefer pairings

for which the magnitude of the corresponding partial disturbance gain, $\|\mathbf{P}_{d1}\|_2 \leq 1$ so that $\|\mathbf{y}_1\|_2 \leq 1$ (by setting $\mathbf{u}_1 = 0$ in eq 30 in the Appendix) at all frequencies even under the worst case where $\|\mathbf{d}\|_2 = 1$. Therefore, to evaluate the feasibility of partial control one must for each choice \mathbf{u}_2 - \mathbf{y}_2 , rearrange the system as in eqs 2 and 3 and calculate \mathbf{P}_{d1} using eq 6.

3. Bioreactor Model

A schematic diagram of a continuous bioreactor is shown in Figure 4. From a chemical engineering point of view it can be viewed as a continuous stirred tank reactor (CSTR) with well-mixed contents and constant volume. The dilution rate (D) and the feed substrate concentration (S_f) are available as manipulated inputs. The cell mass concentration (X) and substrate concentration S are the process state variables, and we assume that X and S are available for controller design. Although this assumption is rarely satisfied in practice, these state variables can often be estimated from secondary variables such as oxygen consumption rate and carbon dioxide production rate.

The most important overall reaction for this study is the growth of one population of microorganisms on a single limiting substrate, namely, *simple microbial growth process* or *single biomass/single substrate process*:



From a reaction engineering point of view this reaction is autocatalytic since the cell mass is a catalyst of its own production as indicated by the feedback arrow \curvearrowright (there is no cell mass growth without initial cell mass added) but is not consumed by the growth reaction. In other words, the rate r (g cells/(h·L)) for formation of new cells increases with cell concentration itself. Usually, the formation rate r is assumed to be proportional to the concentration of cells (X), i.e., $r = \mu(S)X$. We assumed that the specific growth rate (μ (h⁻¹)) is given by the Monod model

$$\mu(S) = \frac{\mu_m S}{K_s + S} \quad (8)$$

where μ_m (h⁻¹) and K_s (g/L) represent the maximum specific growth rate and the saturation constant respectively. The dynamical behavior of the *simple microbial growth process* is most often described by the following "unstructured"² model which is the result of the material balances on the cell mass and the substrate in a constant-volume continuous bioreactor (e.g., Bastin and Dochain, 1990)

$$\frac{dX}{dt} = \mu(S)X - DX \quad (9)$$

$$\frac{dS}{dt} = D(S_f - S) - \frac{\mu}{Y_{XS}} X \quad (10)$$

where Y_{XS} is the yield coefficient [g cells/g substrate] which is assumed constant in this paper.

3.1. Steady-State Behavior. From eqs 9 and 10, the steady state values of cell mass and substrate concentrations are³

$$\frac{dX}{dt} = 0 \Rightarrow \mu(\bar{S}) = \bar{D} \Rightarrow \bar{S} = \frac{K_s \bar{D}}{\mu_m - \bar{D}} \quad (11)$$

$$\frac{dS}{dt} = 0 \Rightarrow \bar{X} = Y_{X/S}(\bar{S}_f - \bar{S}) \quad (12)$$

Here the overbar denotes steady-state values. The effect of \bar{D} and \bar{S}_f on the steady-state values of X and S are shown graphically in Figure 5.

As can be seen from eq 11, the steady-state substrate concentration (\bar{S}) is independent of the feed concentration (\bar{S}_f). From a reaction engineering point of view, this unusual feature is due to the autocatalytic reaction. Thus \bar{S} depends only on the dilution rate (\bar{D}). On the other hand, \bar{X} depends also on \bar{S}_f as given by eq 12. Another phenomenon caused by the autocatalytic reaction is the possibility for washout. Mathematically, washout corresponds to the case when \bar{D} is so high such that the above steady-state equations have no physical solution. Specifically, \bar{X} in eq 12 must be positive; that is, we must require that $\bar{S}_f > \bar{S}$. Inserting this requirement into eq 11, we find that dilution rate \bar{D} must be less than a critical value, D_c , which depends on \bar{S}_f

$$D_c = \frac{\mu_m \bar{S}_f}{K_s + \bar{S}_f} = \mu(\bar{S}_f) \quad (13)$$

Physically, at high dilution rates $\bar{D} > D_c$ (see Figure 5a), the cells cannot grow fast enough to keep up with its dilution, and the culture is washed out of the reactor. Similarly, at the other extreme, at very low but nonzero dilution rates, a large fraction of the cells may die from starvation and then the reaction stops since the limiting substrate is not being added fast enough to permit maintenance of cell metabolism, but this effect is not included in our simple model since no maintenance term is included.

For many continuous bioreactors the objective is to maximize the cell productivity $P = DX$ (g cells/(h·L)). As shown in Figure 5, the productivity increases when S_f increases, but for changes in D it has a maximum value (set $dP/dD = 0$) corresponding to

$$D_{opt} = \mu_m \left(1 - \sqrt{\frac{K_s}{K_s + \bar{S}_f}} \right) \quad (14)$$

The nominal model parameter values and steady-state data for two operating points are given in Table 1. Here operating point No. I is the one studied by Menawat and Balachander (1991), and operating point No. II corresponds to the maximum productivity.

3.2. Linearized Model. Linearizing eqs 9 and 10 around a nontrivial steady state yields the transfer function model

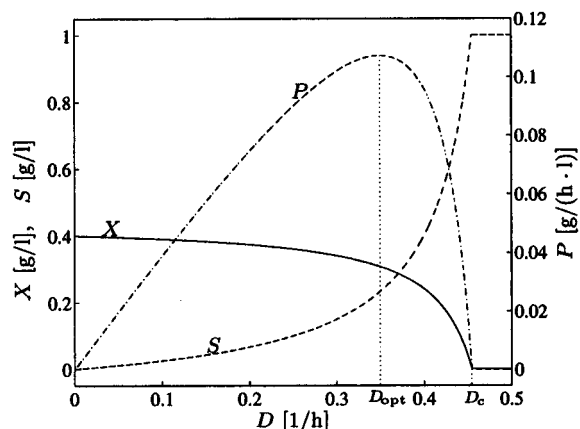
$$\mathbf{y}(s) = \mathbf{G}(s) \mathbf{u}(s) + \mathbf{G}_d(s) \mathbf{d}(s) \quad (15)$$

$$\mathbf{y} = \begin{bmatrix} \Delta X \\ \Delta S \end{bmatrix}, \quad \mathbf{u} = \begin{bmatrix} \Delta D \\ \Delta S_f \end{bmatrix} \quad \left(\text{or } \mathbf{u} = \begin{bmatrix} \Delta D_w \\ \Delta D_S \end{bmatrix} \right) \quad (16)$$

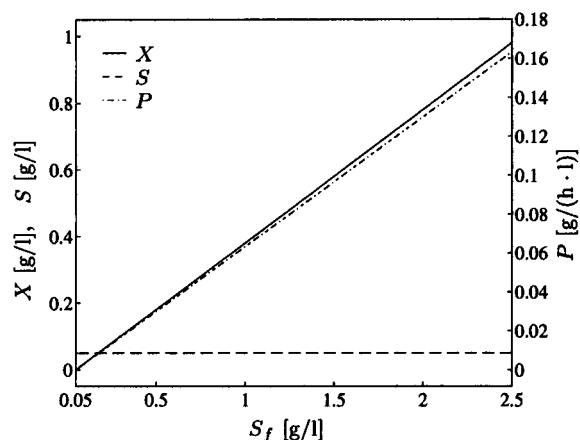
$$\mathbf{d} = [\Delta \mu_m \quad \Delta K_s \quad \Delta Y_{X/S} \quad \Delta D_d \quad \Delta S_{fd}]^T$$

(or $\mathbf{d} = [\Delta \mu_m \quad \Delta K_s \quad \Delta Y_{X/S} \quad \Delta D_{wd} \quad \Delta S_{fd} \quad \Delta D_{sd}]^T$) (17)

where the outputs (states) \mathbf{y} , inputs \mathbf{u} , and disturbances \mathbf{d} represent deviations from the steady state. In addi-



(a) Effect of D with $S_f = 1$ g/l



(b) Effect of S_f with $D = 0.17$ h⁻¹

Figure 5. Steady-state behaviors of X , S , and P as a function of (a) D and (b) S_f . Values of μ_m , K_s , and $Y_{X/S}$ are from Table 1.

Table 1. Steady-State Data

operating point	\bar{D} (h ⁻¹)	\bar{S}_f (g/L)	\bar{X} (g/L)	\bar{S} (g/L)	$\bar{P} = \bar{D}\bar{X}$ (g/(h·L))
No. I	0.17	1.0	0.38	0.05	0.065
No. II	0.35	1.0	0.31	0.23	0.109
washout	>0.46	1.0	0	1.00	0

nominal model parameter		
μ_m (h ⁻¹)	K_s (g/L)	$Y_{X/S}$ (g/g)
0.5	0.1	0.4

tion to possible disturbances in the manipulated inputs D and S_f , we have included disturbances in the model parameters μ_m , K_s , and $Y_{X/S}$ which may stem from variations in the environment conditions such as temperature, pH, aeration rate, etc. The input-output transfer function matrix from

$$\begin{bmatrix} \Delta D \\ \Delta S_f \end{bmatrix} \text{ to } \begin{bmatrix} \Delta X \\ \Delta S \end{bmatrix}$$

is then

$$\mathbf{G}(s) = \begin{bmatrix} \frac{-\bar{X}}{s+a} & \frac{\bar{D}\bar{X}}{(s+a)(s+\bar{D})} \frac{d\mu}{dS} \\ \frac{\bar{X}}{(s+a)Y_{X/S}} & \frac{s\bar{D}}{(s+a)(s+\bar{D})} \end{bmatrix} \quad (18)$$

where

$$a = \frac{\bar{X}}{Y_{X/S}} \frac{d\mu}{dS}$$

Remarks about the Model.

(1) The model is stable at all nontrivial steady states. At washout conditions, $\bar{X} \rightarrow 0$ and the pole $a \rightarrow 0$, so the linearized model approaches instability.

(2) The steady-state gain matrix is obtained by setting $s = 0$. As expected S_f has no steady-state effect on S (see the 2,2-element of $\mathbf{G}(0)$ in eq 18) and therefore should not be used to control S .

(3) Except for this zero gain between S_f and S , neither the transfer function $\mathbf{G}(s)$ nor any of its elements contains RHP-zeros. However, measurement delays in obtaining X or S have not been included which will limit the achievable performance.

(4) Since the yield coefficient $Y_{X/S}$ is assumed constant, one of the eigenvalues is fixed at $-\bar{D}$ irrespective of the reaction, and it can be easily shown that there is a combined state, e.g. $Z = X + Y_{X/S}S$, representing a reaction invariant. We have

$$\frac{dZ}{dt} = \frac{dX}{dt} + Y_{X/S} \frac{dS}{dt} \quad (19)$$

and substituting eqs 9 and 10 into eq 19 then yields

$$\frac{dZ}{dt} = -D(Z - Y_{X/S}S_f) \quad (20)$$

This applies irrespective of the reaction kinetics $\mu(S)$, so Z is indeed a reaction invariant.

(5) From the transfer function matrix the effect of D is first order and does not affect the combined state Z . Thus, the system is not "state controllable" with D as an input. Physically, if D is used to control X (or S) the uncontrollable combined state Z will "drift away" by itself unaffected by the feedback using D because the steady state value $\bar{Z} = Y_{X/S}\bar{S}_f$ is independent of D . Menawat and Balachander (1991) indicated that this may be a problem. However, as pointed out by Agrawal and Lim (1984), it may not have any practical significance since the uncontrollable system is *stable*, so it is possible to design a control system with D as an input where only one output (X or S) is controlled. Any control problems will appear in the controllability analysis of the uncontrolled output. This is the approach taken below.

4. Controllability Study

4.1. Scaling of Variables. The *scaled* transfer matrices are derived by scaling all variables with respect to their maximum allowed changes.

$$\mathbf{G}' = \begin{bmatrix} \overline{\Delta X} & 0 \\ 0 & \overline{\Delta S} \end{bmatrix}^{-1} \mathbf{G} \begin{bmatrix} \overline{\Delta D} & 0 \\ 0 & \overline{\Delta S}_f \end{bmatrix} \quad (21)$$

$\mathbf{G}'_d =$

$$\begin{bmatrix} \overline{\Delta X} & \\ & \overline{\Delta S} \end{bmatrix}^{-1} \mathbf{G}_d \begin{bmatrix} \overline{\Delta \mu_m} & & & & \\ & \overline{\Delta K_s} & & & \\ & & \overline{\Delta Y_{X/S}} & & \\ & & & \overline{\Delta D_d} & \\ & & & & \overline{\Delta S_{fd}} \end{bmatrix} \quad (22)$$

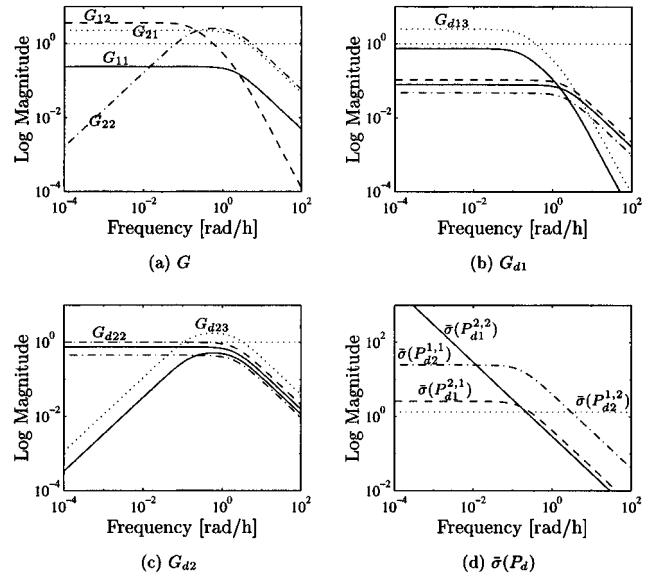


Figure 6. Frequency responses at the operating point No. I.

(In the following the prime (') used to denote the scaled matrices is omitted to simplify notation). The allowed maximum output changes are

$$\overline{\Delta X} = 10\% \bar{X}; \quad \overline{\Delta S} = 20\% \bar{S}$$

The allowed maximum input changes are

$$\overline{\Delta D} = 30\% \bar{D}; \quad \overline{\Delta S}_f = 35\% \bar{S}_f$$

The expected maximum disturbance changes are

$$\overline{\Delta \mu_m} = 10\% \overline{\mu_m}; \quad \overline{\Delta K_s} = 20\% \overline{K_s}; \quad \overline{\Delta Y_{X/S}} = 25\% \overline{Y_{X/S}}$$

$$\overline{\Delta D_d} = 20\% \overline{\Delta D}; \quad \overline{\Delta S_{fd}} = 20\% \overline{\Delta S}_f$$

4.2. Controllability Analysis Results. Operating Point No. I. At this operating point the cell growth is substrate limited. The steady-state gain matrices in terms of scaled variables are

$$\mathbf{G}(0) = \begin{bmatrix} -0.24 & 3.68 \\ 2.25 & 0 \end{bmatrix}$$

$$\mathbf{G}_d(0) = \begin{bmatrix} 0.08 & -0.11 & 2.5 & -0.05 & 0.74 \\ -0.75 & 1 & 0 & 0.45 & 0 \end{bmatrix}$$

The time constants at this operating point are $1/a = 0.5$ h and $1/D = 5.9$ h. The corresponding frequency response plots are shown in Figure 6.

We now proceed with the controllability analysis in order to evaluate the five control configurations by following the controllability analysis procedures described in section 2.

1. Controllability Analysis of Controlled Output. a. Input Constraints. The first requirement is that the open-loop gain, $|G_{ij}|$ for the "controlled pairing" should be larger than the disturbance gains $|G_{dik}|$ to avoid input constraints. We first note that the steady-state gain from S_f to S is zero which means that S_f cannot be used to control S at low frequencies. The steady-state gain from D to X is only -0.24 , whereas the gain for a disturbance in yield ($Y_{X/S}$) is about 2.5. This means that the control action in D needed to reject the largest disturbance in $Y_{X/S}$ (which corresponds to a change in $Y_{X/S}$ of 25%) is about $2.5/0.24 \approx 10$ times

Table 2. P_d at Operating Point No. I

configuration		disturbance				
No.	$u_j \rightarrow y_i$	μ_m	K_s	$Y_{X/S}$	D_d	S_{fd}
1	$D \rightarrow X$	0	0	23.75	0	7
2	$D \rightarrow S$	0	0	2.5	0	0.74
3	$S_f \rightarrow X$	-0.75	1	0	0.45	0
4	$S_f \rightarrow S$	∞	∞	0	∞	0

higher than what is allowed. The conventional turbidostat is therefore not recommended at operating point No. I where the cell growth is substrate limited. This is consistent with the conclusion of Agrawal and Lim (1984).

b. Bandwidth Requirements. From the frequency-dependent plots of the elements in G_d , the bandwidth requirement to achieve acceptable rejection for disturbances in $Y_{X/S}$ (the worst disturbance) is 0.4 rad/h for X (response time of shorter than 2.5 h required) (see the dotted curve marked by G_{d13} in Figure 6b), and 3 rad/h for S (response time of shorter than 0.3 h required) (see the dotted curve marked by G_{d23} in Figure 6c). In practice, this means that it may be favorable to control X if very long measurement delays are expected.

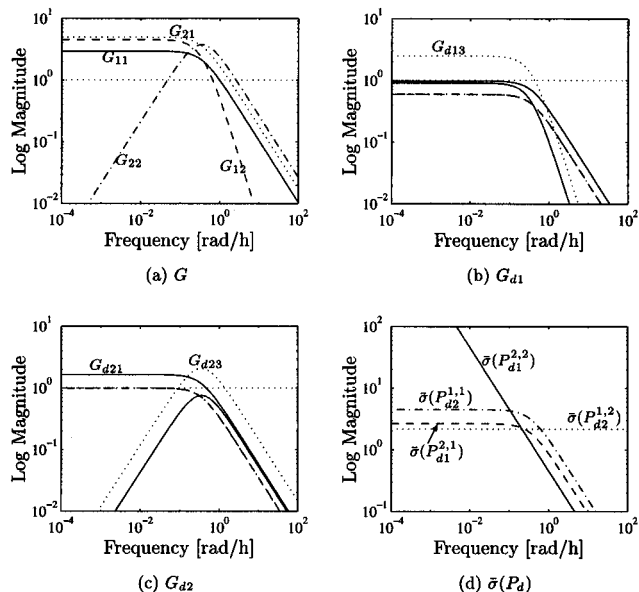
2. Controllability Analysis of Uncontrolled Output. The effect of disturbances on the uncontrolled output are given by the partial disturbance gain. The steady-state values are listed for individual disturbances in Table 2, and the overall effect of simultaneous disturbances on the uncontrolled output, $\|\mathbf{P}_d\|_{\infty} = \bar{\sigma}(\mathbf{P}_d)$, is shown as a function of frequency in Figure 6d where the superscripts i, j of $\bar{\sigma}(P_{dij}^{i,j})$ refer to the controlled output y_i and corresponding input u_j , and the subscript l denotes the uncontrolled output y_l .

From the steady state values in Table 2 and the frequency response of $\bar{\sigma}(\mathbf{P}_d)$ in Figure 6d, the best configuration is the $S_f \rightarrow X$ configuration (see the dotted curve marked by $\bar{\sigma}(P_{d2}^{2,2})$ in Figure 6d). However, the $D \rightarrow S$ configuration (see the dashed curve marked by $\bar{\sigma}(P_{d1}^{2,1})$ in Figure 6d) is better at higher frequencies. The $S_f \rightarrow S$ configuration (see the solid curve marked by $\bar{\sigma}(P_{d1}^{2,2})$ in Figure 6d) is not feasible since the sensitivity to some disturbances is infinite, while the $D \rightarrow X$ configuration (see the dashdot curve marked by $\bar{\sigma}(P_{d2}^{1,1})$ in Figure 6d) is unacceptable with large sensitivity to disturbances in $Y_{X/S}$ (24 times larger than acceptable) and in S_f (7 times larger than acceptable).

If the feed substrate concentration is difficult to manipulate, the $D_w \rightarrow X$ configuration (modified turbidostat) proposed by Agrawal and Lim (1984) is quite effective. The steady-state gain from D_w to X (with D_S constant) is -1.70. The steady-state values of the partial disturbance gain giving the effect of various disturbances on the uncontrolled output S are

$$\begin{bmatrix} d_k \\ P_{d2k}^{l,1} \end{bmatrix} = \begin{bmatrix} \mu_m & K_s & Y_{X/S} & D_{wd} & S_{fd} & D_{Sd} \\ -0.7 & 0.93 & 1.66 & 0 & 0.49 & 0.42 \end{bmatrix}$$

which is almost acceptable. Here $P_{d2k}^{l,1}$ is the partial disturbance gain for the effect of the disturbance d_k on the uncontrolled output y_2 (S) with the output y_1 (X) controlled using the input u_1 (D_w). In particular, we note that the effects of disturbances in $Y_{X/S}$ and in S_f on the uncontrolled output S ($P_{d23}^{1,1} = 1.66$, $P_{d25}^{1,1} = 0.49$) are much less than for the conventional turbidostat ($P_{d23}^{1,1} = 23.75$, $P_{d25}^{1,1} = 7$). Thus, using the dilution rate of the sterile water stream (D_w) to control X gives much better control performance than using the total dilution

**Figure 7.** Frequency responses at the operation point No. II.**Table 3.** P_d at Operating Point No. II

configuration		disturbance				
No.	$u_j \rightarrow y_i$	μ_m	K_s	$Y_{X/S}$	D_d	S_{fd}
1	$D \rightarrow X$	0	0	4.21	0	1.53
2	$D \rightarrow S$	0	0	2.5	0	0.91
3	$S_f \rightarrow X$	-1.65	1	0	0.99	0
4	$S_f \rightarrow S$	∞	∞	0	∞	0

rate (D) (conventional turbidostat). Actually, manipulating the dilution rate of the sterile water stream (D_w) is equivalent to manipulating the effective feed substrate concentration ($S_{ef} = (D_S S_f)/(D_w + D_S)$).

In conclusion, linear controllability analysis results show that the $S_f \rightarrow X$ configuration is best at operating point No. I.

Operating Point No. II. This operating point corresponds to the maximum productivity where the cell growth is not substrate limited. We have

$$\mathbf{G}(0) = \begin{bmatrix} -2.95 & 4.52 \\ 4.97 & 0 \end{bmatrix}$$

$$\mathbf{G}_d(0) = \begin{bmatrix} 0.98 & -0.59 & 2.5 & -0.59 & 0.91 \\ -1.65 & 1 & 0 & 0.99 & 0 \end{bmatrix}$$

The time constants at this operating point are $1/a = 2.3$ h and $1/D = 2.9$ h. The corresponding frequency response plots are shown in Figure 7. We note immediately that the outputs are more sensitive to both inputs and disturbances than at operating point No. I. In particular, this is the case for changes in the dilution rate D where the gain for its effect on relative changes X has increased by more than a factor of 10 (from -0.24 to -2.95). This means that tighter control is needed to reject disturbances in this case, and since the reactor is operating closer to washout, tighter control is needed also to avoid washout.

The steady-state values of the partial disturbance gain are listed in Table 3, and the overall effect of disturbances, $\bar{\sigma}(\mathbf{P}_d)$, is shown as a function of frequency in Figure 7d.

From the steady-state values of the partial disturbance gain, and in particular the frequency response of $\bar{\sigma}(\mathbf{P}_d)$ shown in Figure 7d, the $D \rightarrow S$ configuration (see the dashed curve marked by $\bar{\sigma}(P_{d1}^{2,1})$ in Figure 7d) is preferable; especially at high-frequency range. How-

Table 4. Controller Tunings Used in Figures 8 and 9

line type	configuration	K_c	τ_1 (h)
curves 1	conventional turbidostat ($D \rightarrow X$ configuration)	-2	0.5
curves 2	conventional nutristat ($D \rightarrow S$ configuration)	1	0.5
curves 3	concentration turbidostat ($S_f \rightarrow X$ configuration)	4	4
curves 4	concentration nutristat ($S_f \rightarrow S$ configuration)	4	0.5
curves 5	no control action	0	0

ever, at this operating point there is no big difference in terms of the controllability of these control configurations, except for the $S_f \rightarrow S$ configuration (see the solid curve marked by $\bar{\sigma}(P_{d1}^{2,2})$ in Figure 7d) which is still not feasible. Also the $D \rightarrow X$ configuration (see the dash-dot curve marked by $\bar{\sigma}(P_{d2}^{1,1})$ in Figure 7d) may be efficient.

A more detailed discussion on the $D \rightarrow X$ configuration (conventional turbidostat) is given in the following. For the case when the cell concentration X is perfectly controlled by the dilution rate D , we get

$$\Delta X = \mathbf{G}_{11} \Delta D + \mathbf{G}_{d1k} d_k = 0$$

$$|\Delta D| = \left| \frac{\mathbf{G}_{d1k} d_k}{\mathbf{G}_{11}} \right| \leq \left| \frac{\mathbf{G}_{d1k}}{\mathbf{G}_{11}} \right| < 1, \forall k = 1, \dots, 5,$$

Then even under the maximum disturbance ($d_k = 1$), X can be perfectly controlled by D without encountering input constraint. For the uncontrolled substrate concentration S under a disturbance d_k at the steady state

$$P_{d23}^{1,1} = \frac{\partial S}{\partial Y_{XS}} = 4.21, \quad P_{d25}^{1,1} = \frac{\partial S}{\partial S_f} = 1.53$$

Thus, the effect of the disturbance in Y_{XS} or S_f on the uncontrolled S is much less than in the first case where the growth is substrate limited. Therefore, when the substrate does not limit the cell growth during the fermentation process, the conventional turbidostat is also effective; especially when the disturbances in Y_{XS} and S_f are less important.

5. Simulation Results

In this section we present nonlinear simulation results to confirm the validity of the conclusions from the linear controllability analysis presented in the previous section. All simulations are for operating point No. 1 and a simple PI controller is used for the controlled output. Two alternative control actions are the dilution rate D and the feed substrate concentration S_f , the corresponding control laws are

$$D = \bar{D} + K_c [e(t) + 1/\tau_1 \int_0^t e(t) dt] \quad (23)$$

$$S_f = \bar{S}_f + K_c [e(t) + 1/\tau_1 \int_0^t e(t) dt] \quad (24)$$

where $e(t) = \bar{X} - X$ (or $\bar{S} - S$). Because of the low order of the model (first-order or second-order transfer functions without time delays) considered in our case, ordinary controller tuning techniques, e.g., Ziegler-Nichols method, are not applicable. We therefore set the proportional gain (K_c) to give a manipulated input (control action) of reasonable magnitude and set the integral time (τ_1) to get the acceptable response of the controlled output. The resulting controller tunings are given in Table 4.

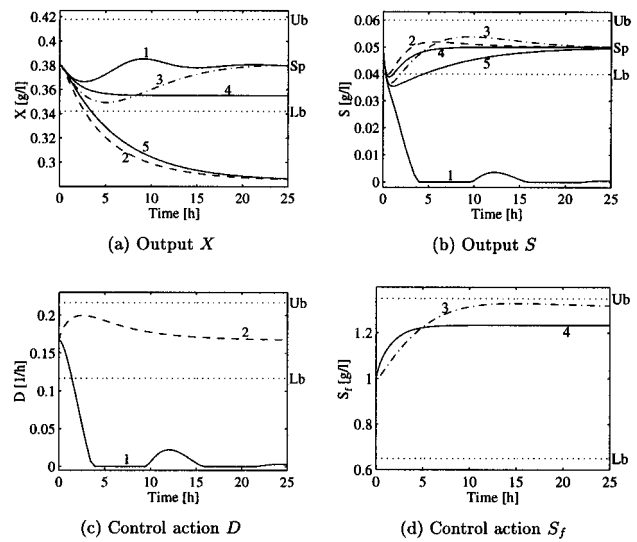


Figure 8. Time responses to a 25% step disturbance in Y_{XS} . Ub = upper bound; Lb = lower bound; Sp = set point.

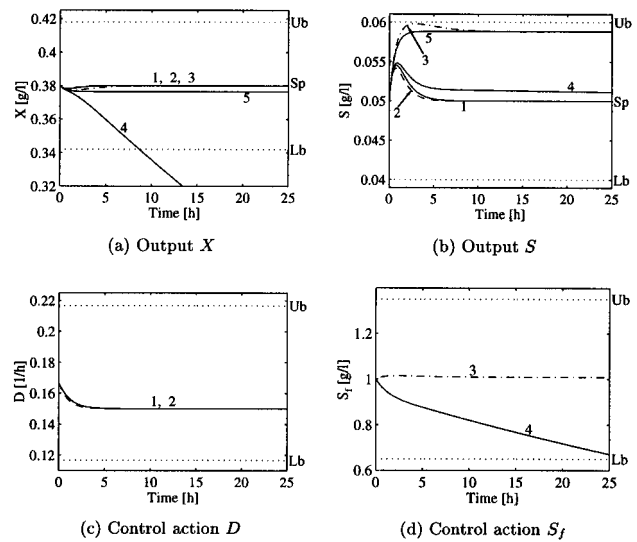


Figure 9. Time responses to a 10% step disturbance in μ_m . Up = upper bound; Lb = lower bound; Sp = set point.

Figure 8 shows step responses to a disturbance of 25% decrease in the yield factor (Y_{XS}) from 0.4 to 0.3 (g/g). Figure 9 shows step responses to a disturbance of 10% decrease in specific growth rate (μ_m) from 0.5 to 0.45.

From the simulations we find:

No control (curves 5): The system cannot be left uncontrolled because of disturbances in Y_{XS} that results in cell concentration exceeding its bound (see Figure 8a).

Conventional turbidostat (curves 1): For a disturbance in Y_{XS} the conventional turbidostat is unacceptable because the uncontrolled output S exceeds its bound. In fact S goes to zero and so does the dilution rate D (see Figure 8b–c), which means there is no production.

Conventional nutristat (curves 2): For a disturbance in Y_{XS} the conventional nutristat is poor because the uncontrolled output X exceeds its bound (see Figure 8a).

Concentration turbidostat (curves 3): Overall, the best performance is obtained by using the concentration turbidostat. This confirms the linear controllability analysis results. We see that with this configuration both the cell concentration and substrate concentration remain within their allowable bounds (as shown in Figures 8a–b and 9a–b) and so does the feed substrate

concentration (S_f) without violating the input constraints (see Figures 8d and 9d).

Concentration nutristat (curves 4): For a disturbance in μ_m the concentration nutristat (curves 4 in Figure 9) is unacceptable because the uncontrolled output X exceeds its bound and eventually the reaction will stop: the input concentration S_f is continuously lowered in order to try to keep S constant. However, because the gain is zero at steady state, it is not possible to keep S constant in the long run, and eventually S_f will reach 0 and the reaction stops (in fact, we may get washout before this occurs since washout occurs when S_f falls below 0.05 g/L; recall the plot in Figure 5b). From the fermentation technology point of view, when a continuous bioreactor is operated at a steady state, the variation in the substrate concentration caused by the feed substrate concentration is exactly balanced or consumed by the growth of cell mass and results in no net change in the substrate concentration in the reactor finally; i.e., S is independent of S_f . On the other hand, S is dependent of the maximum specific growth rate μ_m . Thus the effect of the disturbance in μ_m on S cannot be compensated by changing S_f . Similar results with respect to disturbances in K_s and D are obtained (not shown in the paper). Therefore this control configuration is not feasible in most cases.

A careful comparison shows that *all* these results are consistent with the linear controllability analysis results in the previous section.

6. Conclusions

We have studied alternative control configurations for a *simple microbial growth processes* in continuous bioreactors. At the substrate-limited growth conditions (operating point No. I), the controllability analysis results indicate that using S_f to control X (the concentration-turbidostat) is the best control configuration. This conclusion is consistent with the result of Menawat and Balachander (1991). The conventional turbidostat cannot be used at this operating point because the cell concentration (X) is insensitive to changes in the dilution rate (D). The conventional nutristat is also not recommended from the controllability analysis, and it has the additional problem that it is difficult to accurately measure low values of substrate concentration (Agrawal and Lim, 1984).

At higher dilution rates where the cell growth is not substrate limited (operating point No. II), the conventional nutristat is slightly better than the other configurations, consistent with the results of Agrawal and Lim (1984). However there is no big difference among the first three control configurations. Thus the conventional turbidostat is also effective.

The concentration nutristat where S_f is used to control S (proposed by Menawat and Balachander (1991)) is unacceptable at all operating points because S_f has no steady-state effect on S .

We stress that these results are derived for the *simple microbial growth processes* in a continuous bioreactor. Also, we have not considered the measurement problem which is one of the main obstacles for effective control of bioreactors. However, a number of secondary measurements are often available, such as temperature, pH, CO_2 , and O_2 in the exhaust gas, which may be used to estimate the concentrations of cell mass and substrate.

In this paper, we have in eq 7 generalized the expression for the partial disturbance gain, first pro-

posed by Skogestad and Wolff (1992), to the case with more than one uncontrolled output.

The simulation results are consistent with the linear controllability analysis results. This shows that the partial disturbance gain is an effective tool for controllability analysis. The main advantage with a controllability analysis is that it is independent of controller parameter tuning and makes detailed simulations unnecessary.

Nomenclature

\mathbf{C} = controller transfer function matrix
 D = F/V = dilution rate (h^{-1})
 D_S = dilution rate of the concentrated substrate stream (h^{-1})
 D_w = dilution rate of the sterile water stream (h^{-1})
 d = disturbance
 F = feed flow rate (L/h)
 F_S = flow rate of the concentrated substrate stream (L/h)
 F_w = flow rate of the sterile water stream (L/h)
 \mathbf{G} = plant transfer function matrix
 \mathbf{G}_d = disturbance transfer function matrix
 K_c = controller gain (h)
 K_s = saturation constant in Monod model (g/L)
 P = cell productivity (g cells/(h·L))
 \mathbf{P}_d = partial disturbance gain
 $\|\mathbf{P}_d\|_2$ = induced 2-norm of \mathbf{P}_d
 r = cell growth rate [g cells/(h·L)]
 s = Laplace variable
 S = substrate concentration (g/L)
 S_{ef} = effective feed substrate concentration (g/L)
 S_f = feed substrate concentration (g/L)
 S_{sp} = set point value of S (g/L)
 u = plant input
 V = volume (L)
 X = cell concentration (g/L)
 X_{sp} = set point value of X (g/L)
 $Y_{X/S}$ = yield coefficient (g cells/g substrate)
 y = plant output

Greek Symbols

$\bar{\sigma}(\mathbf{P}_d)$ = largest singular value of \mathbf{P}_d
 τ_1 = integral time (h)
 ω = frequency (rad/h)
 $\mu(S)$ = specific growth rate (h^{-1})
 μ_m = maximum specific growth rate (h^{-1})

Appendix. Derivation of the Partial Disturbance Gain

Consider a linear model of the form

$$\mathbf{y}(s) = \mathbf{G}(s) \mathbf{u}(s) + \mathbf{G}_d(s) \mathbf{d}(s) \quad (25)$$

We here assume that the outputs \mathbf{y}_2 are perfectly controlled by using \mathbf{u}_2 and use the following definition of the partial disturbance gain for the uncontrolled outputs \mathbf{y}_1 :

$$\mathbf{P}_{d1} \stackrel{\text{def}}{=} \left(\frac{\partial \mathbf{y}_1}{\partial \mathbf{d}} \right)_{\{\mathbf{y}_2=0\} \text{ using } \{\mathbf{u}_2\}} \quad (26)$$

As shown in Figure 2, we rearrange and partition the model $\mathbf{y} = \mathbf{G}\mathbf{u} + \mathbf{G}_d\mathbf{d}$ such that the first part of \mathbf{y} contains the uncontrolled outputs (\mathbf{y}_1), and the first part of \mathbf{u} contains the unused inputs (\mathbf{u}_1), whereas the remaining outputs \mathbf{y}_2 are controlled using the remaining inputs \mathbf{u}_2 . We then have

$$\mathbf{y}_1 = \mathbf{G}_{11}\mathbf{u}_1 + \mathbf{G}_{12}\mathbf{u}_2 + \mathbf{G}_{d1}\mathbf{d} \quad (27)$$

$$\mathbf{y}_2 = \mathbf{G}_{21}\mathbf{u}_1 + \mathbf{G}_{22}\mathbf{u}_2 + \mathbf{G}_{d2}\mathbf{d} \quad (28)$$

In order to evaluate the effect of \mathbf{d} on \mathbf{y}_1 when \mathbf{y}_2 is perfectly controlled using \mathbf{u}_2 , we set $\mathbf{y}_2 = 0$ and solve for \mathbf{u}_2 in eq 28 to get

$$\mathbf{u}_2 = -\mathbf{G}_{22}^{-1}\mathbf{G}_{d2}\mathbf{d} - \mathbf{G}_{22}^{-1}\mathbf{G}_{21}\mathbf{u}_1 \quad (29)$$

We have here assumed that \mathbf{G}_{22} is square and invertible, otherwise we may replace \mathbf{G}_{22}^{-1} by the pseudo-inverse, \mathbf{G}_{22}^\dagger . By substituting eq 29 into eq 27 we get

$$\mathbf{y}_1 = (\mathbf{G}_{d1} - \mathbf{G}_{12}\mathbf{G}_{22}^{-1}\mathbf{G}_{d2})\mathbf{d} + (\mathbf{G}_{11} - \mathbf{G}_{12}\mathbf{G}_{22}^{-1}\mathbf{G}_{21})\mathbf{u}_1 \quad (30)$$

The expression of the partial disturbance gain for \mathbf{y}_1 with \mathbf{y}_2 perfectly controlled using \mathbf{u}_2 , is thus (e.g., Havre and Skogestad (1996))

$$\mathbf{P}_{d1} = \mathbf{G}_{d1} - \mathbf{G}_{12}\mathbf{G}_{22}^{-1}\mathbf{G}_{d2} \quad (31)$$

This expression of the partial disturbance gain is general (no assumptions on \mathbf{G}_{11}).

We introduce a matrix $\Delta^{-1} = (\mathbf{G}_{11} - \mathbf{G}_{12}\mathbf{G}_{22}^{-1}\mathbf{G}_{21})^{-1}$ which is called the *Schur complement* of \mathbf{G}_{22} in \mathbf{G} . Assuming \mathbf{G}_{22}^{-1} and Δ^{-1} exist, we have from the matrix inversion lemma (e.g., Zhou, Doyle, and Glover (1996) p 23),

$$\mathbf{G}^{-1} = \begin{bmatrix} \mathbf{G}_{11} & \mathbf{G}_{12} \\ \mathbf{G}_{21} & \mathbf{G}_{22} \end{bmatrix}^{-1} = \begin{bmatrix} \Delta^{-1} & -\Delta^{-1}\mathbf{G}_{12}\mathbf{G}_{22}^{-1} \\ -\mathbf{G}_{22}^{-1}\mathbf{G}_{21}\Delta^{-1} & \mathbf{G}_{22}^{-1} + \mathbf{G}_{22}^{-1}\mathbf{G}_{21}\Delta^{-1}\mathbf{G}_{12}\mathbf{G}_{22}^{-1} \end{bmatrix} \quad (32)$$

With $\mathbf{G}_d = [\mathbf{G}_{d1} \ \mathbf{G}_{d2}]^T$ we may rewrite eq 31 as follows:

$$\begin{aligned} \mathbf{P}_{d1} &= \Delta\Delta^{-1}(\mathbf{G}_{d1} - \mathbf{G}_{12}\mathbf{G}_{22}^{-1}\mathbf{G}_{d2}) = \\ &\quad \Delta(\Delta^{-1}\mathbf{G}_{d1} - \Delta^{-1}\mathbf{G}_{12}\mathbf{G}_{22}^{-1}\mathbf{G}_{d2}) \\ &= ([\mathbf{G}^{-1}]_{11})^{-1}[\mathbf{G}^{-1}\mathbf{G}_d]_1 \end{aligned} \quad (33)$$

For the special case with *one* uncontrolled output \mathbf{y}_1 , \mathbf{G}_{11} and also Δ^{-1} are scalars, and then eq 33 becomes

$$\mathbf{P}_{d1} = \frac{[\mathbf{G}^{-1}\mathbf{G}_d]_1}{[\mathbf{G}^{-1}]_{11}} \quad (34)$$

which is identical to the expression first derived by Skogestad and Wolff (1992), for the case with *one* uncontrolled output.

Literature Cited

- (1) From a scaling point of view, the induced infinity-norm (e.g., Skogestad and Postlethwaite, (1996), p 518) may be preferable. However, in the paper the *overall* effect of *simultaneous* disturbances is mostly concerned. We choose to use the induced 2-norm as it gives the average effect of all elements (disturbances), whereas the induced infinity-norm reflects the worse-case effect (the maximum element or maximum row sum).
 - (2) The term "unstructured" designates that the cell growth can be represented by a single overall reaction, for example, because the fermentation is dominated by a single, homogeneously growing microorganism.
 - (3) For other kinetic schemes, like the substrate inhibition kinetics (Edwards et al., 1972) multiple steady states may exist.
- Agrawal, P.; Lim, H. C. Analysis of various control schemes for continuous bioreactors. *Adv. Biochem. Eng./Biotechnol.* **1984**, *30*, 61–90.
- Bastin, G.; Dochain, D. *On-line Estimation and Adaptive Control of Bioreactors*; Elsevier: Amsterdam, 1990.
- Edwards, V. H.; Ko, R. C.; Balogh, S. A. Dynamics and control of continuous microbial propagators to subject substrate inhibition. *Biotechnol. Bioeng.* **1972**, *14*, 939–974.
- Havre, K.; Skogestad, S. Input/output selection and partial control. *Preprints IFAC '96, 13th World Congress of IFAC*; Pergamon Press: San Francisco, CA, 1996; Vol. M, pp 181–186.
- Menawat, A. S.; Balachander, J. Alternate control structures for chemostat. *AIChE J.* **1991**, *37*, 302–306.
- Skogestad, S.; Morari, M. Control configuration selection for distillation columns. *AIChE J.* **1987**, *33*, 1620–1635.
- Skogestad, S.; Wolff, E. A. Controllability measures for disturbance rejection. *Proc. IFAC Workshop on Interactions Between Process Design and Control*; Pergamon Press: London, UK, 1992; pp 23–29.
- Skogestad, S.; Postlethwaite, I. *Multivariable Feedback Control: Analysis and Design*; John Wiley & Sons: New York, 1996.
- Zhou, K.; Doyle, J. C.; Glover, K. *Robust and Optimal Control*; Prentice-Hall, Inc.: Upper Saddle River, NJ, 1996.

Received for review March 5, 1996
Revised manuscript received October 17, 1996
Accepted October 17, 1996[®]

IE960123L

[®] Abstract published in *Advance ACS Abstracts*, December 1, 1996.